Bull Volcanol (2007) 69:643–659
DOI 10.1007/s00445-006-0100-7

RESEARCH ARTICLE

Imaging and modelling the subsurface structure of volcanic calderas with high-resolution aeromagnetic data at Vulcano (Aeolian Islands, Italy)

Isabel Blanco-Montenegro · Riccardo De Ritis · Massimo Chiappini

Received: 16 August 2005 / Accepted: 13 September 2006 / Published online: 2 December 2006

Abstract In this paper, we present a magnetic model of the subsurface structure of Vulcano island based on high-resolution aeromagnetic data. Three profiles across the most intense magnetic anomalies over the Piano and Fossa calderas were selected for the magnetic modelling, which was constrained by structural and volcanological data, previous geophysical models, paleomagnetic data, and borehole stratigraphy obtained from two deep wells. The interpretation of the magnetic sources represents a significant contribution to the understanding of the Piano and Fossa calderas' underlying structure, providing us with evidence of the lateral discontinuity between them at depth. We propose that the positive magnetic anomalies in the Piano caldera area are caused by: (a) the remnants of an early submarine volcano; (b) an outcropping dyke swarm related to the feeding system of the Primordial Vulcano phase (beneath Mt. Saraceno); and (c) the presence of a non-outcropping dyke system intruded along a NE–SW-oriented intra-caldera fault (beneath the eastern part of the Piano caldera). Offshore, to the west, the magnetic anomaly map suggests the presence of a submarine volcanic structure, not revealed by bathymetric data, which could represent the eruptive centre, the presence of which has been indirectly deduced from the outcrop of eastern-dipping lavas on the western seashore. Magnetic modelling of the Fossa caldera points to the presence of a highly magnetized cone-like body inside the Fossa cone, centred beneath the oldest crater rims. We interpret this body as a pile of tephritic lavas emplaced in an early phase of activity of the Fossa cone, suggesting that the volume of mafic lavas that erupted at the beginning of the construction of the Fossa edifice was more significant than has previously been deduced. Furthermore, the presence of a magnetized body inside the Fossa cone implies that high temperatures are contained in very limited spaces, do not affect its bulk inner structure, and are restricted to fumarolic conduits and vents. In addition, structures beneath the western and northern part of the Fossa caldera are revealed to have null or low magnetization, which can be ascribed to the presence of pyroclasts and hyaloclastites in this area as well as to a large volume of hydrothermally altered materials. This suggests that the hydrothermal system, with a very limited extension at present, affected a larger area in the past, especially beneath the western part of the caldera.

Keywords Potential field modelling · High-resolution aeromagnetic data · Crustal imaging · Calderas · Volcanic islands · Vulcano · Aeolian Islands

Editorial responsibility: M. Ripepe

I. Blanco-Montenegro (✉)
Dep. de Física, Escuela Politécnica Superior,
Universidad de Burgos,
Avda. de Cantabria s/n,
09006 Burgos, Spain
e-mail: iblanco@ubu.es

R. De Ritis · M. Chiappini
Istituto Nazionale di Geofisica e Vulcanologia,
Via di Vigna Murata 605,
00143 Rome, Italy

Introduction

Magnetic anomaly maps are a powerful tool for the investigation of the subsurface structure of volcanic areas because of the high magnetic response of volcanic rocks. The interpretation of magnetization contrasts revealed by such maps, in the light of the existing geological and geophysical knowledge, can provide valuable information on the inner structure of a volcano, thus contributing to a better understanding of its evolution (i.e. Lénat et al. 2001; Blanco-Montenegro et al. 2003). Airborne acquisition of magnetic data is particularly useful, as it provides regular coverage, thereby ensuring satisfactory sampling of magnetic anomalies, but it also enables the characterization of geological structures located in unattainable areas such as submerged portions of volcanic islands. Moreover, recent improvements in navigation and data acquisition have enhanced the possibilities of aeromagnetic research, making it possible to acquire high-resolution magnetic data, which are especially suitable for mapping shallow geological features (Finn and Morgan 2002).

The island of Vulcano is an active volcanic system located in the Aeolian archipelago (southern Tyrrhenian Sea). It represents a unique site for volcanological research due to its complex volcanic evolution, which has produced a large variety of products (ranging in composition from tephrites and shoshonites to trachytes and rhyolites) erupted in an area of a few square kilometres and has also formed two calderas. Vulcano has been extensively studied from a geological, geochemical, and geophysical point of view, and its recent volcanic history is reasonably well understood (i.e. De Astis et al. 1997 and references therein). However, its earlier magmatic phases, the products of which are buried under younger volcanics, are almost unknown. Previous geophysical studies in this area focused on large-scale structures of the Aeolian arc (Barberi et al. 1994) or, when devoted to a detailed study of Vulcano, provided information on the subsurface structure mainly beneath the central part of the island (Budetta et al. 1983; Chiarabba et al. 2004).

In 1999, an aeromagnetic survey was conducted by the Geological Survey of Austria, and a magnetic anomaly map of Vulcano and southern Lipari was published by Supper et al. (2004). In 2005, the area was resurveyed by the *Istituto Nazionale di Geofisica e Vulcanologia* of Italy (INGV) with a different profile orientation that extended the survey area by up to about 4 km to the west of the island. The purpose of this high-resolution, low-altitude survey was to characterize the shallow inner structure of this volcanic island, both in the subaerial and submarine portions.

In this paper, we present the results of the quantitative modelling of the aeromagnetic data referred to above. The main purpose of this study is to improve our knowledge of the subsurface structure of the volcanic edifice of Vulcano, especially beneath the Fossa caldera, where the present volcanic activity is concentrated, as well as the Piano caldera. The magnetic modelling was accomplished by means of a forward approach and was constrained by paleomagnetic, borehole, and geological data.

Geological and geophysical setting

The Aeolian Islands and the Vulcano-Lipari-Salina alignment

The Aeolian archipelago lies on the south-eastern side of the Tyrrhenian Sea, between the Sicilian–Calabrian continental margin and the Tyrrhenian basin. It comprises seven islands and several seamounts forming a ring-shaped structure, interrupted in the central sector by the NW–SE alignment of the islands of Vulcano, Lipari, and Salina (Fig. 1). Aeolian volcanism displays a wide compositional range over time, with products belonging to the calc-alkaline, high-K calc-alkaline, shoshonitic, and alkaline potassic associations. As you move in an anticlockwise direction from NW to SE along the Aeolian ring, the volcanic activity is progressively younger (Barberi et al. 1974; Keller 1982).

The regional geodynamic environment represents the transition from the thickened raising crust of the Apennine belt to the thinned Tyrrhenian crust affected by subsidence. Xenoliths found on the islands prove the presence of metamorphic and sedimentary formations belonging to the Calabro-Peloritano arc below the volcanic edifices (Barberi et al. 1994 and the references therein). The Aeolian Islands and the Tyrrhenian plain are considered to be a volcanic arc and a back-arc basin, respectively, related to the subduction of the African plate below the southernmost part of the Italian peninsula (Keller 1974; Ellam et al. 1989; Barberi et al. 1994; De Astis et al. 1997).

From the structural point of view, extensional tectonics affected the pre-volcanic basement, articulated in lows and highs oriented along a NNW–SSE direction. The Vulcano–Lipari–Salina ridge lies inside a graben-like structure that lowered the crystalline basement down to depths of 3,000–3,600 m (Barberi et al. 1994). The ridge develops along two main systems of NW–SE-trending right-lateral strike-slip faults, parallel to a regional tectonic feature outcropping in northern Sicily, known as the Tindari–Letojanni fault, which represents the northward propagation of the regional lithospheric discontinuity of the Malta escarpment (Ventura et al. 1999; Fig. 1). This element intersects the NE–SW and E–W features that controlled the Plio-Quaternary evolution of the whole southeastern Tyrrhenian margin (Gabbianelli et al. 1991).

Structural features and volcanic evolution of Vulcano

The Vulcano–Lipari–Salina alignment is a submarine volcanic ridge that rises 1,000 m from the continental slope lying on continental crust. Vulcano is the southernmost island of this ridge, with an emerged extension of about 22 km^2 and two intersecting calderas as its most noteworthy

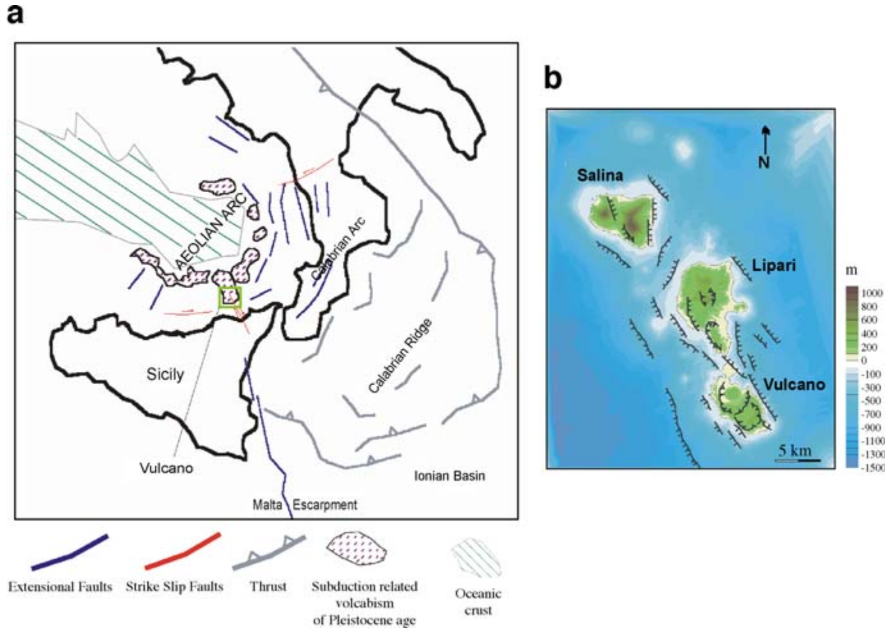

Fig. 1 **a** Geodynamical framework of the Aeolian volcanism, showing the location of Vulcano island (*green square*); **b** Structural scheme of the Salina, Lipari, Vulcano ridge (modified from Favalli et al. 2005 and Ventura et al. 1999)

morphological features. Due to the lack of caldera-forming eruption products, these calderas (known as Vulcano del Piano and La Fossa) have been interpreted as structural depressions produced by tectonic activity.

Several subaerial composite volcanic structures can be recognized at present on the island (Fig. 2): the Primordial Vulcano, Vulcano del Piano or the Piano caldera, the Fossa caldera, the Fossa cone, the Lentia complex, and Vulcanello (i.e. Keller 1980; De Astis et al. 1989; Gabbianelli et al. 1991). Regarding the early phases of submarine activity, very little information is available. The outcrop of a succession of eastern-dipping lavas in stratigraphic discordance on the western seashore (Spiaggia Lunga) suggests the presence of an older volcano—now totally eroded—to the west of the known subaerial eruptive centres (Keller 1980).

Subaerial activity at Vulcano started 120 ka ago with the formation of a stratovolcano known as the Primordial Vulcano, whose products (trachyandesitic and trachybasaltic lavas, dykes, and pyroclastic deposits) outcrop in the southern half of the island. This phase of activity extended up to 98 ka ago. The intracalderic activity of the Vulcano del Piano arose from the collapse of the Primordial Vulcano. The products of this phase involved both the inner and outer caldera structure with the appearance of volcanic centres along the caldera-rim faults (97–78 ka) and, subsequently (50 ka), in the form of intra-caldera vents related to N–S and NE–SW fractures (Timpone del Corvo and Passo del Piano). A thick sequence of lava flows (150–170 m) filled the caldera depression, followed by pyroclastic and scoriae deposits (Gioncada and Sbrana 1991). The Piano caldera in-fill products are mostly shoshonitic basalts and leucite-bearing tephrites (Keller 1980; De Astis et al. 1989).

In the time interval between 50 and 20 ka, tectonic activity formed the southern border of the Fossa caldera. Between 78 and 15.5 ka, a pyroclastic trachybasaltic phase took place in the area of the Fossa caldera and Vulcanello with the emplacement of blanket scoriae and hydromagmatic deposits. Intercalated with these units is a series of thick pyroclastic deposits of hydromagmatic ash and lapilli.

As the remnant of a wider volcanic structure, today, the Lentia complex testifies to volcanic activity that took place after the trachybasaltic phase in the northwestern part of Vulcano island between 24 and 15 ka. In this period, rhyolitic to trachytic lava flows and minor domes were emplaced along N–S-trending fractures (Ventura 1994). The Lentia complex was involved in the collapse between 15.5 and 7.3 ka that originated the Fossa caldera depression (Gillot et al. 1990). The inner stratigraphy of the Fossa caldera can be reconstructed by means of two drillings carried out on the western and northern side of the Fossa cone (Gioncada and Sbrana 1991; a detailed description of the drillings will be given in the next subsection). The Fossa caldera depression was filled by a thick sequence of pyroclastic products and lavas erupted between 15 and 8 ka in a shallow submarine environment. These products show a high compositional variation covering the whole range from shoshonites to trachytes. This volcanic phase ended with the strombolian activity of Mt. Saraceno in the western part of the island (De Astis et al. 1997).

After the emplacement of leucite-tephritic (lc-tephritic) lavas in the eastern sector of the Fossa caldera (Punta Roja), a composite cone, 391-m high, grew in the last 5.5 ka in the

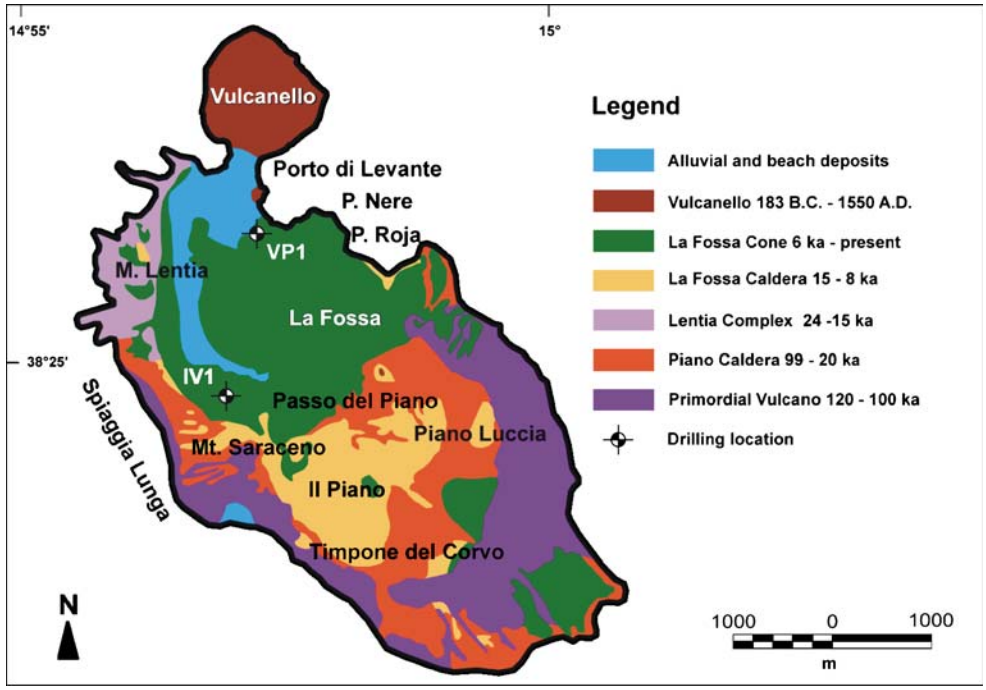

Fig. 2 Simplified geological map of Vulcano, modified from De Astis et al. 1997. The place names mentioned in the text and the location of the two deep wells drilled in the Fossa caldera are shown

centre of the depression. This cone, mainly made up of pyroclastic deposits and minor lava flows, has shifted its activity from NE to SW, as testified by the presence of several rims, which become younger as you move from the NE (Punte Nere–Punta Roja) towards the actual crater. The outcropping deposits are trachytic to rhyolitic in composition (Gioncada and Sbrana 1991). The Fossa cone is still active nowadays.

Vulcanello, the northernmost structure of the island, began its activity as a new island in 183 B.C. and experienced historic eruptions in the sixth and sixteenth centuries (De Astis et al. 1997). It consists of a composite lc-tephritic lava platform and three nested pyroclastic cones.

At a local scale, the structural pattern of Vulcano is characterized by three main sets of faults: NW–SE, N–S, and NE–SW (Ventura 1994; Mazzuoli et al. 1995; Fig. 1b). The NW–SE fractures are related to the regional Tindari–Letojanni fault system, whereas NE–SW and N–S normal faults affect the main structural features bordering the caldera depressions (Gabbianelli et al. 1991; Ventura 1994). The geometrical relationships between these fault systems, the inner depressions, and the analysis of the stress field suggest a structural association related to a pull-apart basin (Gioncada and Sbrana 1991; Ventura 1994). The structural features controlled the migration of volcanic activity over time from SE to NW (with respect to the Primordial Vulcano, the Piano caldera, and the Fossa caldera phases) and the N–S direction of the latest phases (the Fossa cone and Vulcanello; Frazetta et al. 1983). Seismic data have highlighted a different morphology of the western and eastern Vulcano offshores (Gabbianelli et al. 1991). The former is characterized by a quaternary erosion shelf, whereas canyons, escarpments, fractures, and ridges, controlled by NE–SW faults, characterize the latter.

Regarding the plumbing system of Vulcano, the petrographic characteristics of the outcropping units underline an evolving magmatic composition over time (De Astis et al. 1997 and references therein). Initial tectonic movements allowed the uprising of undifferentiated magmas from deeper feeding zones, and subsequent continuous movements controlled magma evolution through a complex interplay between melting processes at the crust–mantle boundary and fault geometries (Mazzuoli et al. 1995). The oldest volcanic phases (the Primordial Vulcano and the Piano caldera) were fed by mafic to intermediate magmas, which later evolved at a high-standing level where they were affected by differentiation processes (Lentia complex). In the subsequent phases, basaltic magmas were not able to reach the surface, with the consequent emplacement of shallow reservoirs and the occurrence of low-volume eruptions of intermediate composition (the Fossa caldera; De Astis et al. 1997).

Previous studies on the subsurface structure of Vulcano

The Aeolian Islands have been studied in the past from a geophysical point of view. The first works published in the 1970s (i.e. Bonasia et al. 1973; Iacobucci et al. 1977) sought to characterize the large-scale structures. Among such works, a regional aeromagnetic and gravimetric study of the Aeolian archipelago is of great interest, which revealed that the Salina–Lipari–Vulcano magmatic axis developed in a deep graben completely filled by volcanic deposits and intrusive bodies (Barberi et al. 1994). Beneath these materials, the crystalline basement appears to be almost non-magnetic.

Drilling carried out by the Italian National Petroleum Company AGIP for geothermal purposes provided very valuable information on the subsurface structure beneath the Fossa caldera (Faraone et al. 1986). The two boreholes drilled inside the caldera (Fig. 2) point to the occurrence of a differential collapse that peaks (~1,000 m) in the northern area (Gioncada and Sbrana 1991). This collapse also affected the southern part of Lipari and seems to relate to extensional tectonics that occurred along the Tindari–Letojanni wrench fault, a conclusion that is also supported by seismic data (Ventura 1994). The lowered area was later affected by intense submarine volcanic activity, resulting in thick beds of hyaloclastites and lava flows that filled the depression before the recent Fossa cone and Vulcanello phases of activity. At a depth of about 1,300 m, the well IV1 penetrated a monzodioritic intrusive body ascribed to the trachybasaltic phase with an estimated age of 30 ka (Fig. 3). This well encountered rapidly increasing temperatures from approximately 1,140 m (112°C) to the bottom at 2,050 m, where the temperature exceeded 419°C. A second well was drilled, which deviated towards north and reached a vertical depth of 1,578 m, with a lateral shifting of 458 m. This hole found a temperature of 243°C at 1,338 m and between 350 and 400°C at the bottom (Faraone et al. 1986).

Since the last eruption that occurred in 1888–1890, the Fossa cone has shown fumarolic activity, particularly intense in the 1920s and from 1978 up until the present (Barberi et al. 1991). Nowadays, a high-temperature fumarolic field, reaching temperatures of over 400°C, has developed inside and on the northern part of the crater, whereas low-temperature fumarolic emissions ($T \leq 100$°C) are present outside the Fossa cone, in the Baia di Levante area (Fulignati et al. 1999). Geochemical and geophysical data clearly demonstrate the existence of an active hydrothermal system beneath the Fossa caldera, at depths of between 500 and 1,000 m bsl (i.e. Chiodini et al. 1992; Berrino 2000).

A detailed gravity survey of Vulcano was carried out by Budetta et al. (1983) to study the shallow structure of the island. The most noteworthy anomaly is a gravity high inside the Piano caldera ascribed to a rising discontinuity between superficial loose pyroclastics and more compact underlying materials (pyroclasts and/or lavas). Unfortunately, the cover-

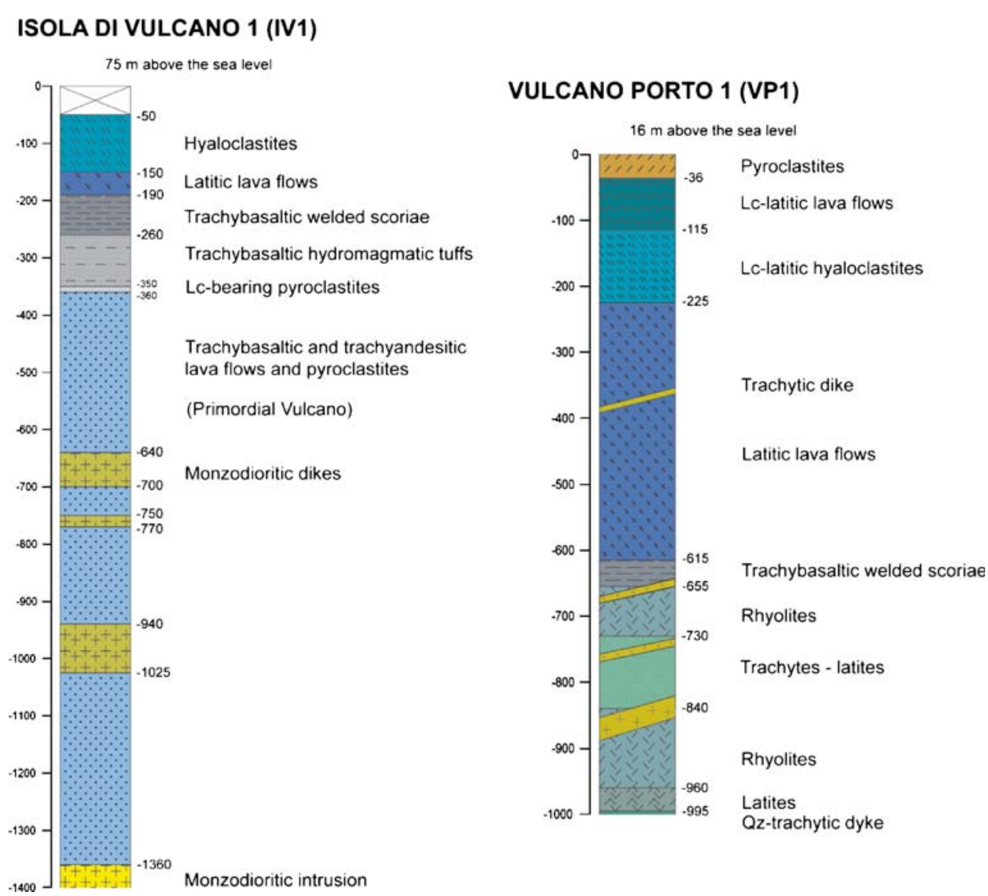

Fig. 3 Stratigraphic columns from the two deep wells drilled in the Fossa caldera (adapted from Gioncada and Sbrana 1991). The location of the boreholes is shown in Fig. 2

age of gravity stations is poor or absent in some critical areas such as the Fossa cone and Mt. Saraceno, and therefore, the interpretation of this data set is limited.

A recent seismic investigation aimed at characterizing the shallow structure of Vulcano (Chiarabba et al. 2004) revealed some low-velocity anomalies corresponding to caldera-filling products (pyroclastics, tuffs, lava flows, and hyaloclastites), whereas high-velocity anomalies represent intrusive bodies and lava piles, especially inside the Piano caldera.

High-resolution positive magnetic anomalies were recently interpreted as related to the presence of crystallized feeding systems, intrusions, and buried vents. The alignments of these anomalies show good correspondence with the strikes of regional and local faults in the area, demonstrating that the growth of Vulcano has been strongly controlled by the NW–SE, Tindari–Letojanni strike-slip faults and by the associated N–S striking normal faults that affect this part of the Aeolian archipelago (De Ritis et al. 2005).

Rock magnetic properties

Due to their high content of magnetic minerals, volcanic rocks register high magnetization values that are the source of intense magnetic anomalies. For the purposes of interpreting and modelling the magnetic anomaly map of a volcanic area, it is important to gather together all available paleomagnetic data that provide direct knowledge of the magnetic properties of the outcropping volcanic units.

The great variety of volcanic products erupted at Vulcano during its entire history, which range in composition from tephrites and shoshonites to trachytes and rhyolites and have very different textures that correspond to lava flows, domes, pyroclastic deposits, etc., implies great heterogeneity in rock magnetic properties on this island. To characterize the magnetization intensity of the different geological units, we have used data collected by Zanella and Lanza (1994), Zanella et al. (1999, 2001), and Zanella (2004, personal communication) to estimate average magnetization values for the sampled outcrops. It is important to note that most of the paleomagnetic studies carried out at Vulcano were not intended to characterize the magnetic response of every outcropping volcanic unit but rather to investigate the paleosecular variation of the geomagnetic field (Lanza and Zanella 2003) and to study the magnetic properties of pyroclasts to determine eruptive and emplacement dynamics and set the chronostratigraphic relationships of the sampled deposits (Zanella et al. 1999, 2001). For this reason, some units have been extensively studied, whereas others have not been studied at all. For instance, among the deposits pertaining to the Fossa cone, only the lavas have been sampled, whereas no paleomagnetic information on the pyroclastic deposits of this eruptive phase is available.

Table 1 shows the values of remanent, induced, and total magnetization for the sampled units, as well as their Koenigsberger ratio, that is, the ratio between remanent and induced magnetization. It is important to note that magnetic properties are quite variable, even among samples from the same site. To quantify this variability, the standard deviation of the paleomagnetic measurements was calculated, and it shows the wide range within which rock magnetization values are comprised. Another limitation is linked to the fact that paleomagnetic sampling is always restricted to outcropping units, whereas the magnetic anomaly map is made up of the magnetic fields created mainly by buried structures. In fact, the main aim of this work is to model the subsurface structure of Vulcano, for which no paleomagnetic measurements are available. For these reasons, it is not possible to assign an absolute magnetization value for each lithology, and the paleomagnetic results should be considered as guidance to constrain the magnetic response of the volcanic structures during the magnetic modelling.

In spite of these limitations, some conclusions can be drawn from the paleomagnetic data shown in Table 1. The highest magnetization values correspond to the lc-tephritic lavas of Vulcanello, followed by the lava flow of Punta Roja, with a similar degree of evolution. The less magnetic lava flows are those of rhyolitic and trachytic composition of the Lentia edifice and the Fossa cone, whereas lavas of the Primordial Vulcano show intermediate magnetization values. Finally, trachytic and rhyolitic ash deposits of the Fossa caldera show the lowest total magnetization values in the island.

Regarding the direction of remanent magnetization, and taking into account that the age of Vulcano is of the order of 10^5 years, the secular variation effects of the geomagnetic field are expected to have been averaged. The mean paleomagnetic direction at Vulcano for the last 135 ka is given by D=9.4°, I=53.2° (Lanza and Zanella 2003). This direction differs from the geocentric axial dipole direction D=0°, I=57.8°, a fact that might be ascribed to a long-term, non-axial-dipolar magnetic field component.

Magnetic data

The magnetic data used in this work were collected during the airborne campaign carried out in 2005, aimed at investigating the onshore part of Vulcano and the marine sector up to a distance of about 4 km to the west of the island. Profiles were oriented in the NE–SW direction and were spaced out at intervals of 250 m.

The airborne platform consisted of a cesium magnetometer towed 30 m below a helicopter, a differential global

Table 1 Summary of rock magnetic properties at Vulcano, compiled using the paleomagnetic data provided by Zanella (2004, personal communication)

Eruptive stage	Type of deposit	Lithology	J_R (A m^{-1})	k (SI×10^{-6})	J_I (A m^{-1})	Q	J_{TOT} (A m^{-1})	No. of sampled sites
Primordial Vulcano	Lava flows	Trachybasalts, trachyandesites	2.9±1.5	32,000±12,000	1.1±0.4	2.6	4.0±1.9	18
Piano caldera	Lava flows	Shoshonites	4.0±2.3	27,000±14,000	1.0±0.5	4.0	5.0±2.8	5
		Basalts	1.5	47,720	1.7	0.9	3.2	1
		Leucite–tephrites	4.2±2.8	20,000±5,000	0.7±0.2	6.0	4.9±3.0	5
	Scoriae	Shoshonites, basalts, latites	4.9±3.3	18,000±11,000	0.6±0.4	8.2	5.5±3.7	23
Lentia	Lava flows and domes	Rhyolites	2.5±1.0	23,000±12,000	0.8±0.4	3.1	3.5±1.3	5
	Lava flows	Trachytes	2.8	21,970	0.8	3.5	3.6	1
		Latites	5.4±0.8	11,000±3,000	0.4±0.1	13.5	5.8±0.9	2
La Fossa caldera	Pyroclasts	Trachytes, rhyolites	0.6±0.4	14,500±1,800	0.5±0.1	1.2	1.1±0.5	11
La Fossa cone	Lava flows	Trachytes	2.7±0.7	14,000±3,000	0.5±0.1	5.4	3.2±0.8	2
		Leucite–tephrites (Punta Roja)	5.8	25,200	0.9	6.4	6.7	1
Vulcanello	Lava flows	Leucite–tephrites	6.9±2.7	46,000±3,000	1.6±0.1	4.3	8.5±2.8	5

J_R is natural remanent magnetization, k is bulk magnetic susceptibility, J_I is induced magnetization (calculated assuming an ambient magnetic field of 35 A m^{-1}), J_{TOT} is total magnetization (calculated on the assumption that J_R and J_I are parallel), and Q is the Koenigsberger ratio. When more than one site was sampled, both the average value and the standard deviation are displayed.

positioning system, and a laser altimeter. Total intensity magnetic field data were collected at a sampling rate of 10 Hz, maintaining a clearance of about 150 m above the ground. A base station, consisting of a proton precession magnetometer, was deployed at Vulcanello to record and subsequently remove the external magnetic field variations from the survey data.

The processing of the magnetic data set can be summarized as follows: (a) removal of external field variations; (b) reduction to the geomagnetic epoch 2001.0, using the L'Aquila Geomagnetic Observatory (Central Italy) datum as the reference value; (c) subtraction of the Italian Geomagnetic Reference Field at epoch 2001.0 (De Santis et al. 2003) from the reduced data to remove the main magnetic field; (d) merging and interpolation of the reduced magnetic anomaly data sets on a 120-m cell grid; (e) removal of residual errors by directional cosine and Butterworth filtering of the anomaly grid. In Fig. 4, we show the resulting magnetic map, which represents the anomaly field on a rugged surface approximately following the topography with an average clearance of 150 m from the terrain.

Analysis and modelling of the aeromagnetic anomalies

The magnetic anomaly map of Vulcano shows a complex pattern, with intense anomalies characterized by different wavelengths both over the subaerial and submarine portions of the island (Fig. 4). In particular, the two calderas show a very different magnetic response, pointing to a lateral discontinuity between them at depth. To obtain a magnetic model of the subsurface structure beneath the Piano and the Fossa calderas, we have applied some interpretative techniques that are described in the following paragraphs.

Reduction to the pole

The dipolar nature of magnetic anomalies makes magnetic interpretation difficult, especially when the effects of adjacent sources overlap. The transformation referred to as reduction to the pole (Baranov and Naudy 1964) removes this difficulty, transforming each dipolar anomaly into a positive or negative anomaly and shifting it to the vertical of its source.

As with every interpretative technique, reduction to the pole requires the assumption of some restrictive hypotheses. Thus, the obtention of a reliable and realistic result depends on whether those hypotheses constitute a suitable representation of reality or not. In particular, most reduction-to-the-pole algorithms assume that both the ambient magnetic field and the magnetization have constant directions along the studied area, which must be known in advance.

In the case of Vulcano, the size of the surveyed area allows us to assume a constant direction for the ambient magnetic field. In addition, the age of the island (135 ka for

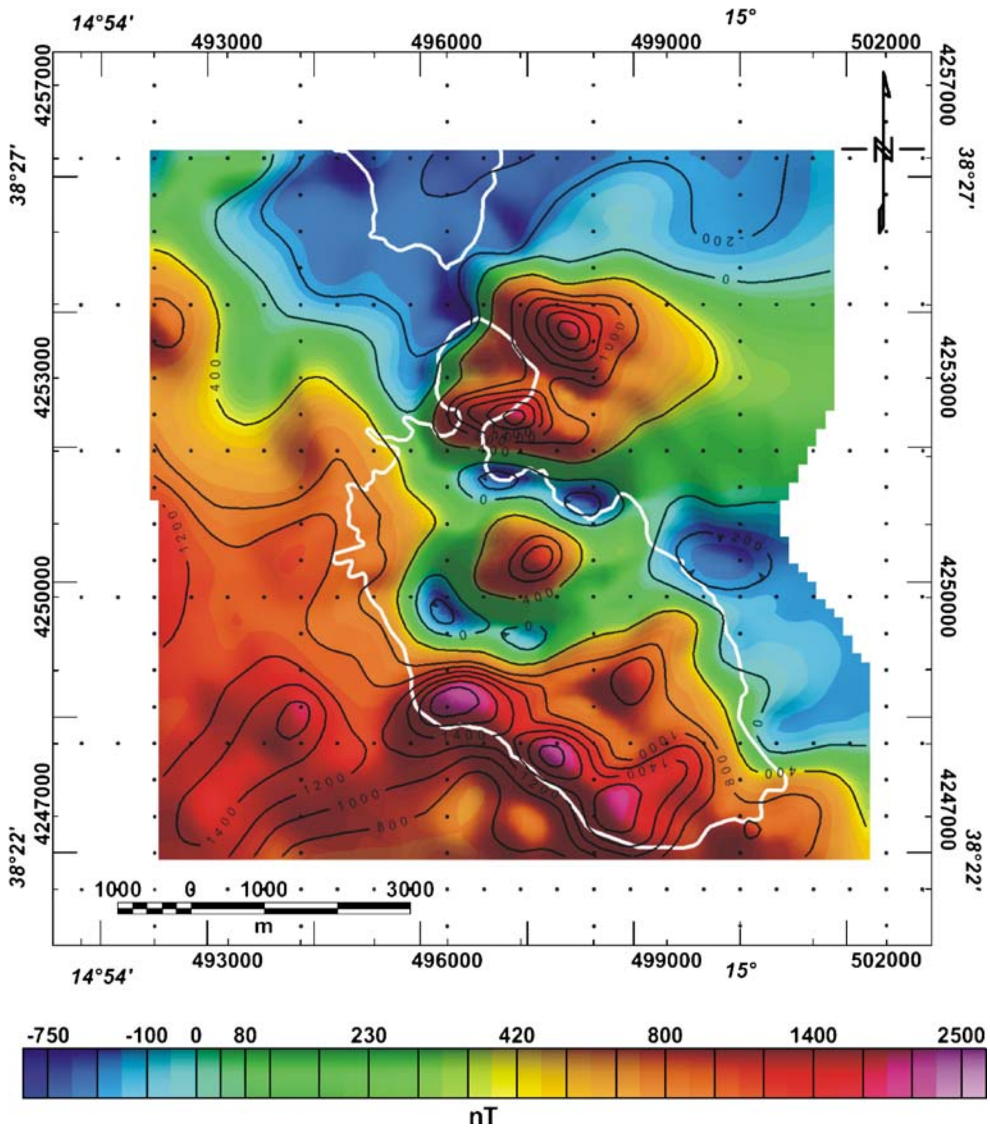

Fig. 4 Aeromagnetic anomaly map of Vulcano island and offshore

the oldest subaerial volcanics) implies that only normal polarities are present. Finally, paleomagnetic studies provide an average direction for the outcropping units of D=9.4°, I=53.2° (Lanza and Zanella 2003). This direction is sufficiently close to the ambient field direction (D=0°, I=57.8°) to allow us to consider that induced magnetization is almost parallel to the remanent component. This assumption is also supported by the fact that the Koenigsberger ratio for Vulcano rocks is high, so the remanence is much more intense than induced magnetization for most rocks on this island. It is also important to note that, when the acquisition of remanent magnetization spans periods of time of the order of 10^5 years or more, variations in the magnetization direction due to the secular variation of the main magnetic field are averaged, and the resulting bulk magnetization direction is parallel to the axial dipole field (except where tectonic movements have occurred). Moreover, magnetic anomalies are practically insensitive to differences in the magnetization direction below 5–10°, so differences between the actual magnetization direction and the direction assumed for the application of reduction to the pole do not substantially affect the resulting reduced-to-the-pole magnetic anomaly map.

We have therefore assumed that for the magnetic modelling of the subsurface structure of Vulcano, the difference in direction between induced and remanent magnetization is negligible, and that the total magnetization vector may be considered parallel to the mean paleomagnetic direction at Vulcano over the last 135 ka (D=9.4°, I=53.2°). Actually, we have also calculated the reduced-to-the-pole anomaly map considering that both the ambient field and the magnetization directions are given by the International Geomagnetic Reference Field. The resulting map is almost identical to the one calculated with magnetization direction based on paleomagnetic data. Therefore, the horizontal location of magnetic contacts in the model would not be substantially affected. The main advantage of using the reduced-to-the-pole anomaly is that it considerably simplifies magnetic modelling when it is accomplished from a forward approach.

The reduced-to-the-pole aeromagnetic anomaly map of Vulcano island and offshore, as well as the topography and bathymetry of the area under study, is shown in Fig. 5. In this map, the different magnetic responses of the two calderas, each reflecting a different subsurface structure, become more evident. In particular, the Piano caldera is characterized by several magnetic highs partially correlated with the caldera rim, whereas the Fossa caldera seems to be less magnetic, with only a short-wavelength positive magnetic anomaly over the eastern part of the cone. In Fig. 5b, the anomalies selected to accomplish the modelling have been identified.

Forward modelling

The final goal of every potential field survey is to obtain some quantitative information about the sources and interpret them in light of the geological knowledge of the area. In this work, we have chosen a forward approach to perform this quantitative modelling. Although 3D modelling might seem ideal for modelling magnetic anomalies, in practice, the complexity of the magnetic pattern in active volcanic areas makes 3D modelling a very challenging task. In most situations, if 2.75D modelling is carried out with care and if supported by previous geological models, it can provide reasonable solutions that improve our knowledge of the crustal structure under study. Moreover, it is important to bear in mind that the final purpose is to gain some information about the geometry and depth of the sources responsible for the main magnetic anomalies by constraining the magnetization values within an interval that is based on available paleomagnetic or petrological data. This is the approach that we have adopted for the magnetic modelling of the subsurface structure at Vulcano. It means that the proposed model must not be considered as an exact solution that accurately represents the structure of the volcanic system but as a model in which the magnetization values and the geometries of the buried bodies will inevitably differ at least to some extent from reality.

Target magnetic sources depend on the geometrical parameters that define the aeromagnetic grid (e.g. height and spatial resolution). Thus, when magnetic data are acquired at a distance of several kilometres from the surface, magnetic anomalies from deep and large sources are enhanced with respect to those linked to shallow structures, whereas high-resolution near-surface magnetic data contain much more information on outcropping bodies and shallow buried structures. The magnetic surveys carried out at Vulcano and offshore belong to the second category, so the estimated depth of the base of the volcanic edifice was considered for the construction of the magnetic models, which is to say structures down to a depth of about 1,000 m bsl (Gabbianelli et al. 1991; Favalli et al. 2005).

The selection of the profiles for the magnetic modelling was done taking into account the main anomalies displayed on the magnetic maps (Figs. 4 and 5b) and paying special attention to the Fossa and the Piano calderas. In particular, a profile across Mt. Saraceno and the Piano caldera was chosen (profile AA') to model the sources of MS and PL positive anomalies. A second profile (profile BB') across the anomalies LF and FC of the Fossa caldera was also selected. Finally, a third N–S profile, which intersects the other two and coincides with a seismic tomography model published by Chiarabba et al. (2004), was considered. To simplify the modelling process, we have chosen to work with the reduced-to-the-pole anomalies (Fig. 5b). As we have discussed in "Reduction to the pole," the age, size, and paleomagnetic characteristics of Vulcano make it possible to obtain a reliable reduced-to-the-pole magnetic anomaly map. Nevertheless, it is important to bear in mind that if actual magnetization differs from the assumed magnetization direction at a specific location, the source position will be slightly shifted from the vertical of the anomaly, although we expect this would not significantly change the main results of this study.

The magnetic modelling was performed with an implementation of a 2.75D forward modelling technique based on the expressions obtained by Talwani and Heirtzler (1964) and Rasmussen and Pedersen (1979) and the algorithm proposed by Won and Bevis (1987). In both profiles, the outcropping structures were constrained by the available surface geology data (Keller 1980). In addition, the subsurface structure beneath the Fossa caldera (profile BB') was constrained by the results of the deep drillings carried out at the Fossa caldera, as shown in Fig. 3 (Gioncada and Sbrana 1991). Rock magnetic properties measured by Zanella (2004, personal communication) and reported in Table 1 were taken into account for the magnetic characterization of the different volcanic units. The proposed models, shown in Figs. 6, 7, and 8 and in Table 2, will be discussed in the following section.

Interpretation and discussion

Subsurface structure beneath the Piano caldera and Mt. Saraceno

To model the subsurface structure beneath the Piano caldera, we have chosen profile AA' because it intersects

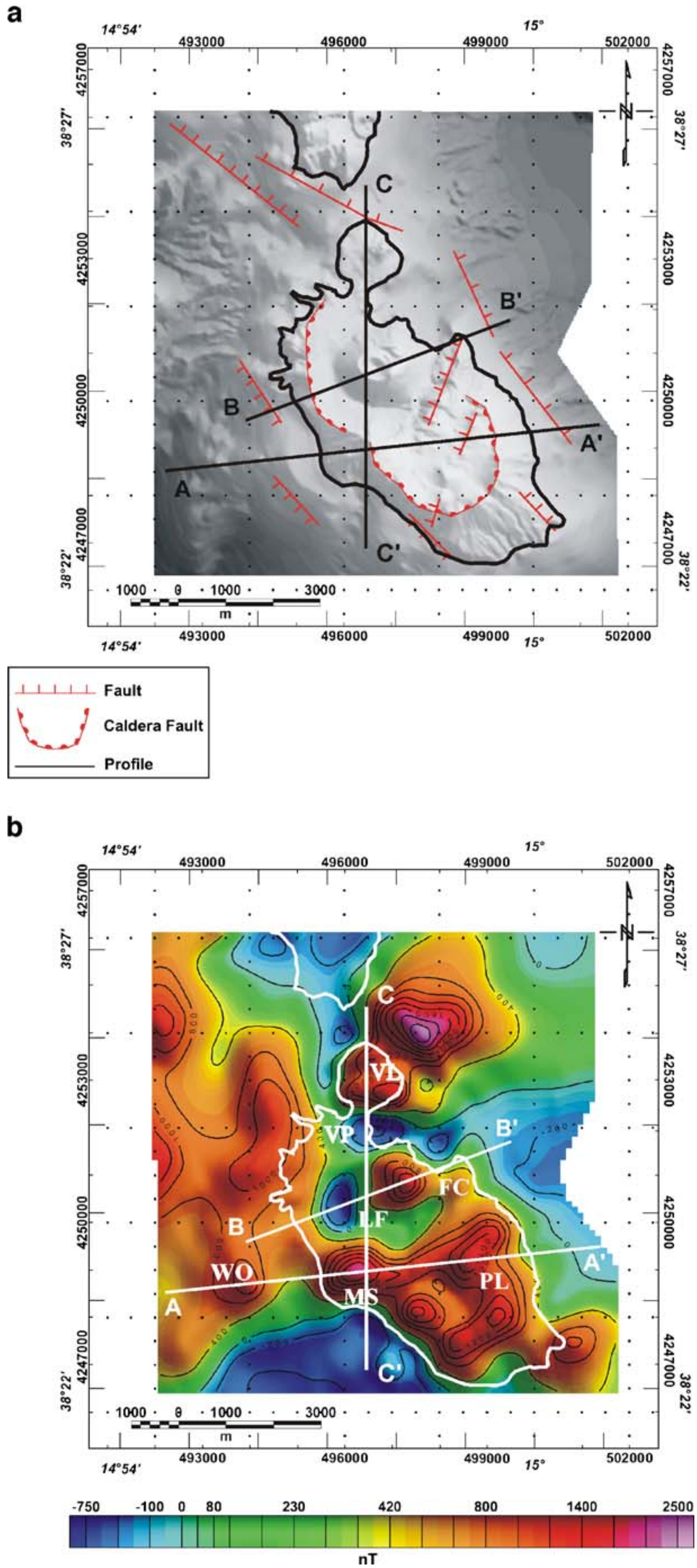

Fig. 5 **a** Digital elevation model of Vulcano island and offshore, showing the main faults; **b** Reduced-to-the-pole aeromagnetic anomaly map of Vulcano and offshore. Magnetic anomalies selected for the modelling are identified with capital letters: *WO* west offshore, *MS* Mt. Saraceno, *PL* Piano Luccia, *FC* the Fossa cone, *LF* the Fossa caldera, *VP* Vulcano Porto, *VL* Vulcanello. The profiles chosen for the modelling have been superimposed on both maps

the most intense anomalies displayed in this area, particularly anomaly MS, located over Mt. Saraceno, and anomaly PL, located over the area called Piano Luccia inside the Piano caldera (see Fig. 5). The profile was extended to the west to model the source of anomaly WO and therefore contribute to the understanding of the structure to the west of the caldera. The construction of the model shown in Fig. 6 was carried out bearing in mind previous knowledge on the structure of this part of Vulcano. Total magnetization values assigned to the different bodies were chosen in accordance with available paleomagnetic measurements (see Table 1). The shallow structure beneath the Piano caldera was constrained by surface geology data (Keller 1980).

The magnetic pattern over the Piano caldera is characterized by a series of magnetic highs, which are among the strongest anomalies of the survey (anomalies MS and PL in Fig. 5b). Although some of them are spatially correlated with the caldera rim, the quantitative modelling of these anomalies demonstrates that they cannot be explained by the morphological effect of the caldera depression. This means that buried magnetized structures are present in this area. We interpret the deepest sources of these positive anomalies as the remnants of an old volcanic edifice corresponding to the initial submarine stage in the formation of Vulcano, the central part of which has been altered due to the collapse of the caldera and later intra-caldera activity (Fig. 6; Table 2). The magnetic highs displayed to the southeast of MS and PL anomalies (Fig. 5b) lead us to think that the remnants of the early submarine volcano extend below the whole of the southern half of the island. This old structure would have been covered later by the materials of the Primordial Vulcano, which was the first subaerial phase of activity at Vulcano. In the area of Mt. Saraceno, the outcrop of a dyke system that cuts the materials of the Primordial Vulcano suggests to us that the positive anomaly is also contributed to by this strongly magnetized structure, which could represent the feeding system of the Primordial Vulcano in this area (Figs. 6 and 8). An interesting result of the magnetic modelling is that the northern and southern limits of this dyke system coincide with two caldera faults, also shown by Chiarabba et al. (2004) in their N–S profile. It is also worth noting that anomaly MS is the most intense magnetic high over the island. Its location represents a key point in the evolution of Vulcano, not only because the two calderic structures intersect at Mt. Saraceno, but also because its volcanic history ranges from the initial activity of the Primordial Vulcano (and, probably, of the previous submarine edifice) to recent mafic activity that occurred about 8 ka ago.

Regarding anomaly PL, the modelling process accomplished within the framework of the existing volcanological knowledge of the area led us to conclude that the main source of this positive anomaly is a strongly magnetized body with a vertical geometry. In particular, we have

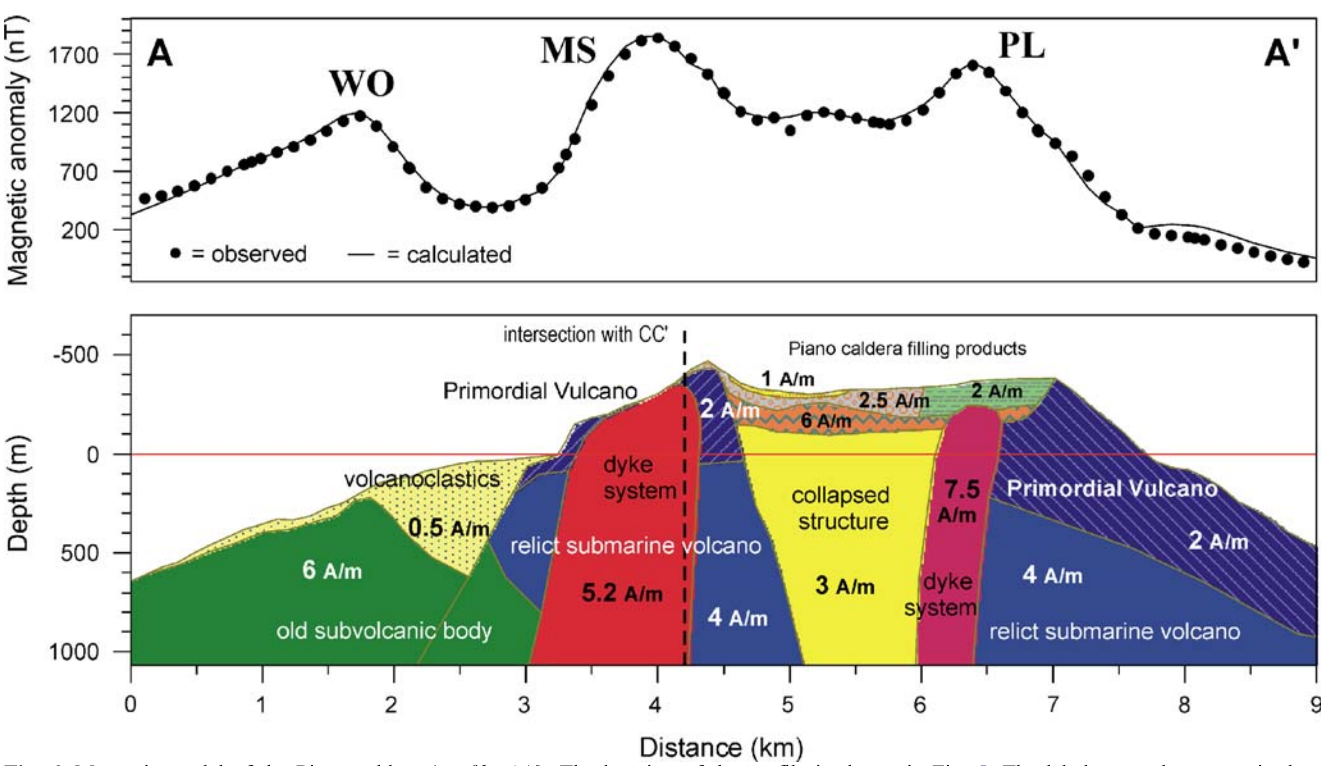

Fig. 6 Magnetic model of the Piano caldera (*profile AA'*). The location of the profile is shown in Fig. 5. The labels over the magnetic data indicate the anomalies identified in Fig. 5b. The size of the bodies in the direction *perpendicular* to the profile is reported in Table 2

verified that a shallow source would imply an overly high magnetization value in comparison with the available paleomagnetic data. We interpret this source as a dyke system whose emplacement could have related to a NE–SW striking volcano-tectonic feature present in this area (see Fig. 5a). The fact that anomaly PL is elongated in that direction supports this interpretation. Contrary to the dyke system of Mt. Saraceno, the dykes inside the Piano caldera do not outcrop, and it is worth noting that their identification has been made possible indirectly through the modelling of their magnetic response. In addition, the intrusion of this dyke system along an intra-caldera fault provides a constraint on the age of this event, which clearly occurred after the caldera collapse. This dyke system and the eastern part of the remnant submarine volcano mentioned before could represent the high-velocity body found by Chiarabba et al. (2004) inside the Piano caldera. However, a direct comparison between the magnetic and the seismic models is difficult due to the different resolution of the models and to the fact that the physical magnitudes they reflect are not necessarily correlated.

Anomaly WO, located offshore to the west of Vulcano, has been interpreted as being due to the products of a buried old volcanic vent. Although bathymetric evidence of the presence of this body is lacking, the magnetic anomaly map clearly shows that a volcanic structure exists beneath this area. Moreover, the presence of an emission centre to the west of Mt. Saraceno has been deduced from the outcrop on the seashore of eastward-dipping lavas that could represent the remnants of an older volcano (Keller 1980; Gioncada and Sbrana 1991). The relative magnetic low between anomaly WO and anomaly MS could be explained by a depression between these two volcanic edifices, favoured by the normal fault that affects this area, and filled by a large volume of almost non-magnetic materials. These materials could be mainly interpreted as volcanoclastic sediments and also as pyroclastites pertaining to the subsequent phases of volcanic activity. The other positive anomalies in the marine area to the west of Vulcano could have a similar origin (see De Ritis et al. 2005).

Finally, it is interesting to mention the magnetic low to the south of Mt. Saraceno, partly intersected by profile CC’. The extremely high magnetic gradient in this area can be only reproduced in the model with an almost vertical contact between the lavas pertaining to the submarine volcano phase and very weakly magnetized materials whose origin will require further investigation in the future.

Subsurface structure beneath the Fossa caldera

The Fossa caldera is the area where present volcanic activity concentrates at Vulcano. It therefore represents a key area in which to perform a detailed modelling of its subsurface structure. In fact, the reduced-to-the-pole aeromagnetic map (Fig. 5b) shows two magnetic anomalies at the Fossa: a negative anomaly over the western part of the caldera

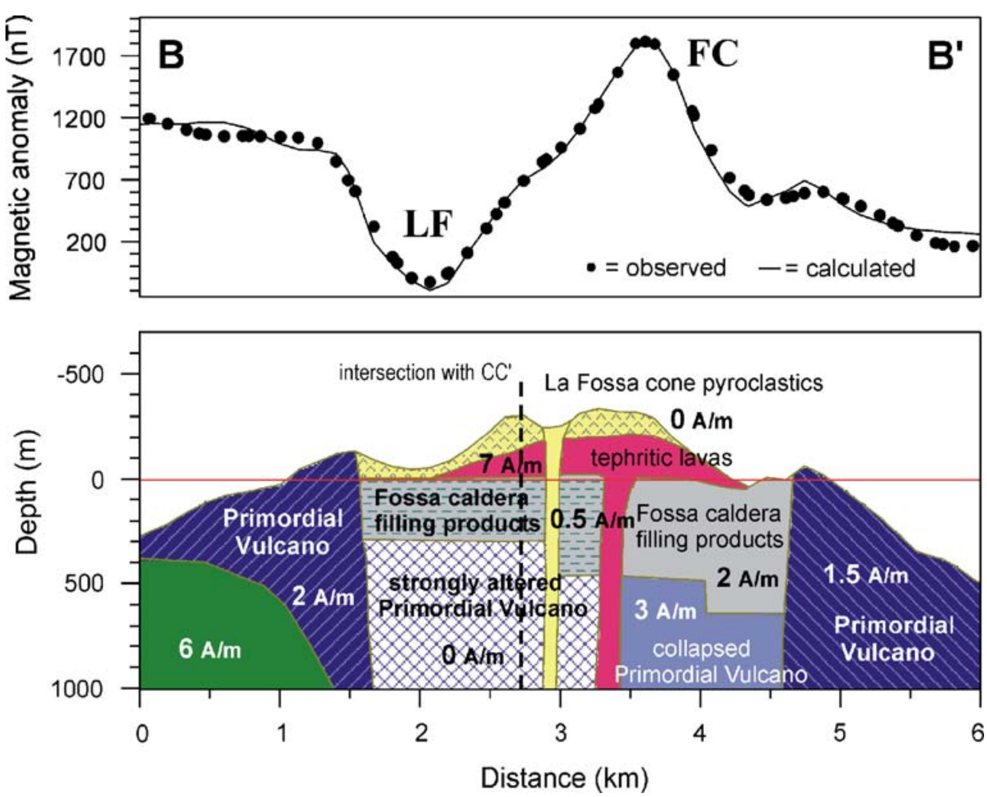

Fig. 7 Magnetic model of the Fossa caldera along *profile BB’*. The location of the profile is shown in Fig. 5. The labels over the magnetic data indicate the anomalies identified in Fig. 5b. The size of the bodies in the direction *perpendicular* to the profile is reported in Table 2

(anomaly LF) and a positive anomaly over the eastern part of the cone (anomaly FC). In addition, in the northern limit of the caldera, a second negative anomaly is displayed (anomaly VP).

Profile BB' was chosen with the purpose of modelling the sources of anomalies LF and FC (Figs. 5 and 7). On the other hand, profile CC' was used to better constrain the subsurface structure beneath the Fossa caldera (Figs. 5 and 8). Although this profile does not intersect anomaly FC by its maximum value, it has the advantages of being coincident with one of the seismic tomography profiles published by Chiarabba et al. (2004) and passing very close to the two deep wells drilled in this area.

The subsurface structure beneath the Fossa caldera was constrained with the data obtained from these boreholes (Figs. 2 and 3). In particular, beneath the western part of the caldera (borehole IV1), the drilling evidenced the presence of a large volume of hyaloclastites under the Fossa cone, pyroclastic deposits and alluvium, a sequence of materials associated with the trachybasaltic phase and finally, the lavas and scoriae pertaining to the Primordial Vulcano phase. The drilling carried out in the northeastern part of the caldera (borehole VP1) revealed a ~500-m-thick sequence of hyaloclastites and submarine lavas that filled the caldera and the presence of rhyolitic–latitic materials from a depth of 640 m bsl. The important differences between the sequences found by the two wells suggest the existence of a fracture somewhere inside the caldera to explain this discontinuity.

The process of forward modelling along profile BB' has provided us with valuable information on the sources of anomalies LF and FC (Figs. 5 and 7). Anomaly FC could be related a priori with the tephritic lavas outcropping at Punta Roja (see Fig. 2). In fact, paleomagnetic samples from these lavas have a total magnetization of about 7 A m^{-1} (Zanella, 2004, personal communication). Assigning this value to the magnetization of the source and assuming that the cone is nonmagnetic because it is made up of

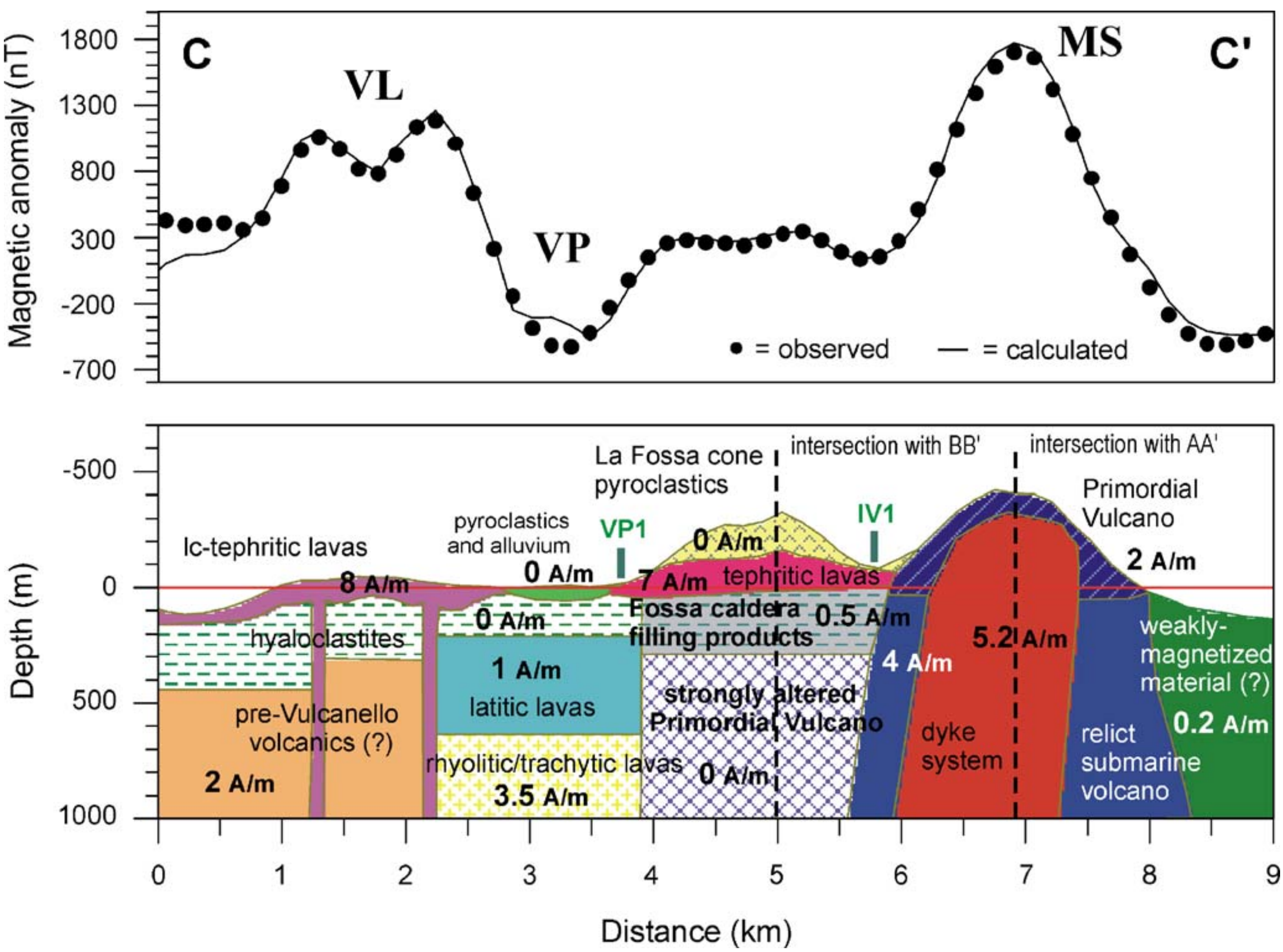

Fig. 8 Magnetic model of the Fossa caldera along *profile CC'*. The location of the profile is shown in Fig. 5. The labels over the magnetic data indicate the anomalies identified in Fig. 5b. The location of the two deep wells drilled inside the Fossa caldera is shown in *green* (see also Fig. 2). The size of the bodies in the direction *perpendicular* to the profile is reported in Table 2

Table 2 Size of the bodies displayed in the models shown in Figs. 6, 7, and 8

Body	y_1 (km)	y_2 (km)
Profile AA'		
Primordial Vulcano:		
Western part	0.6	0.4
Eastern part	4	2
Piano caldera in-fill products:		
Lc-tephritic lavas (orange)	1	0.7
Scoriae (grey)	0.3	0.2
TGR pyroclastics (yellow)	0.5	0.3
Scoriae (green)	0.5	0.5
Old subvolcanic body	1	2
Volcanoclastics	1	1
Relict submarine volcano:		
Western part	0.6	1
Eastern part	2.4	1.2
Collapsed structure	2	1
Mt. Saraceno dyke system	0.6	0.4
Piano Luccia dyke system	0.2	0.2
Profile BB'		
Primordial Vulcano:		
Western part	2	0.5
Eastern part	4	0.3
La Fossa cone pyroclastics	1	1
La Fossa cone tephritic lavas	0.6	1
Tephritic vertical conduit	0.1	0.1
La Fossa caldera in-fill products:		
Western part	0.6	1.5
Eastern part	1	1.5
Strongly altered Primordial Vulcano	0.6	1
Collapsed Primordial Vulcano	1	1
Old subvolcanic body	3	0.6
Profile CC'		
Vulcanello lc-tephritic lavas	0.5	0.5
Vulcanello feeding conduits:		
Northern conduit	0.1	0.1
Southern conduit	0.05	0.3
Hyaloclastites	1	1
Pre-Vulcanello volcanics (?)	2	2
Latitic lavas	2	2
Rhyolitic/trachytic lavas	2	2
La Fossa cone pyroclastics	0.7	0.7
La Fossa cone tephritic lavas	0.3	1.5
Fossa caldera in-fill products	1.2	0.7
Strongly altered Primordial Vulcano	1.2	0.7
Primordial Vulcano	0.6	1
Dyke system	1	0.1
Relict submarine volcano	1.3	0.7
Weakly magnetized material (?)	1	0.3

The strike of the structures is 90° for profiles AA' and BB' and 85° for profile CC'. The variable y_1 is the length towards the south in profiles AA' and BB' and towards the west in profile CC', whereas y_2 is the length towards the north in profiles AA' and BB' and towards the east in profile CC'.

pyroclasts and minor felsic lava flows, we have verified that the source of anomaly FC is located at a shallow depth beneath the cone, and that its geometry is of the type modelled in Fig. 7. This result would imply the existence, beneath and inside the present Fossa cone, of an older cone-shaped body that could be interpreted as a pile of tephritic lava flows. This would suggest that the volume of mafic lavas that erupted at the beginning of the construction of the Fossa edifice was of greater importance than previously deduced from the outcropping deposits. The emission conduits of the Fossa edifice have migrated from NE to SW, and the fact that the magnetic high is centred over the remnants of the oldest craters supports this interpretation. In addition, it should be stressed that borehole VP1 penetrated a series of lc-latitic lava flows at a very shallow depth (see Fig. 3). Although some authors consider that lava flow at La Roja pertains to a volcanic phase before the formation of the Fossa cone (see Ventura et al. 1999 and references therein), the magnetic modelling suggests that this lava flow represents the outcrop at the surface of the source of anomaly FC. Therefore, our result would imply that La Roja lavas represent the earliest stage of the growth of the Fossa cone. Approximately in this area, seismic tomographic data evidenced a shallow high-velocity body, interpreted as the Fossa cone lavas (Chiarabba et al. 2004). It is likely that we are detecting the same structure.

At present, the Fossa cone shows a high-temperature fumarolic field that reaches temperatures of more than 400°C. This fumarolic activity appears on the more recent crater and in the northern sector of the edifice. It might therefore be thought that the inner structure of the Fossa edifice is affected by a thermal anomaly related to the circulating fluids. Nevertheless, the magnetic model demonstrates that the cone is not demagnetized. In fact, the presence of a positive magnetic anomaly over the eastern part of the Fossa cone implies that high temperatures are contained in very limited spaces, do not affect its bulk inner structure, and are restricted to fumarolic conduits and vents.

The vertical sequence beneath the Fossa caldera included in the magnetic modelling is based on the borehole data of Gioncada and Sbrana (1991). The magnetic modelling of the negative anomaly LF revealed that beneath the western part of the Fossa caldera, volcanic structures are nonmagnetic. This could be explained, in part, by the presence of pyroclasts at the surface and by the large volume of hyaloclastites that filled the caldera. However, the existence of an active hydrothermal system is also an important feature to be considered, not only because of the high temperatures at depth related to the circulating fluids, but also because hydrothermal alteration may destroy the magnetite and titanomagnetite of volcanic rocks, drastically reducing their magnetization (Ade-Hall et al. 1971). The absence of magnetic properties at depth beneath the western part of the caldera, deduced from the magnetic modelling, also relates to the materials of the Primordial Vulcano affected by the collapse and found at a depth of about 300 m bsl. This is consistent with the analysis of samples from this unit recovered in the drilling sequence of borehole IV1, which showed that these lavas and scoriae are strongly altered (Gioncada and Sbrana 1991).

Models of the present hydrothermal system beneath the Fossa caldera locate it beneath the Fossa cone and consider that it has a very limited extension, with an estimated volume of less than 0.1 km^3 (Italiano et al. 1984). The lack of magnetic properties in a large area beneath the western part of the caldera, deduced from the magnetic modelling, could be interpreted as a result of hydrothermal alteration that occurred in the past, suggesting that the hydrothermal system is now less developed. In fact, the drillings show that temperature at 1 km reaches a value of approximately 100°C (Faraone et al. 1986), and this means that the demagnetization of the structures pertaining to the volcanic edifice cannot be simply explained as a consequence of present thermal anomalies.

Contrary to what happens in the western part of the Fossa caldera, materials beneath the eastern part of the caldera seem to be magnetized, as deduced from the fitting of magnetic anomalies in this area. This result may indicate that the hydrothermal system was less developed below this area, as is also suggested at present by the lack of fumarolic fields.

Profile CC' (Figs. 5 and 8) has allowed us to model, in addition, the sources of anomalies VP and VL. Again, we have constrained the subsurface structure using the vertical sequences revealed by the drillings. In the model, we have placed the discontinuity between these two sequences below the northern limit of the cone, in the place where Gioncada et al. (2003) locate a normal fault.

Anomaly VP is displayed over the northern limit of the caldera. Beneath this area, borehole VP1 found a large volume of hyaloclastites, which, due to their glassy nature, can be assumed to be almost non-magnetic. In addition, the surface is covered by alluvial deposits and pyroclasts (see Fig. 2) that have been also considered in the model as a layer with zero magnetization. Furthermore, this area is affected by fumarolic activity. Therefore, the circulation of hydrothermal fluids and the subsequent alteration they produce would also contribute to the lack of magnetic properties that is necessary to explain the presence of this magnetic anomaly low. Chiarabba et al. (2004) locate in this area a low-velocity structure interpreted as due to the presence of low-rigidity materials (pyroclasts, hyaloclastites, etc.) that practically coincide with the source of magnetic anomaly VP.

The value of total magnetization assigned in the model to the latitic lavas found by borehole VP1 beneath the hyaloclastitic layer is much lower than the one reported in Table 1 for this type of rock but necessary to fit magnetic anomalies in this area. This difference can be explained by the fact that the value of Table 1 was obtained from samples of only two sites and corresponds to subaerial lava flows of the Lentia complex, whereas the structure of the model represents a lava pile that (a) was emplaced in a different environment (below the sea level) and (b) could have decreased its magnetization due to alteration related with hydrothermal activity. In fact, samples from these lavas have a vitrophyric texture and show incipient alteration (Gioncada and Sbrana 1991). Therefore, the magnetic modelling would suggest that this alteration affects a substantial volume of submarine latitic lavas.

Vulcanello peninsula consists of a lava platform, mainly of lc-tephritic composition, and some pyroclastic cones. Samples of these lavas show the highest magnetization values of the island (see Table 1). We have modelled the positive anomaly over this area (anomaly VL in Fig. 5b, consisting of two adjacent magnetic highs), as mainly due to the outcropping lava flows and the volcanic conduits that fed this mafic activity. We propose that the location of the southernmost feeding conduit corresponds with a fault that marks the northern limit of the Fossa caldera. Beneath these lc-tephritic lavas, we have assumed that there is a thick pile of hyaloclastites, as suggested by Gioncada and Sbrana (1991). However, and because there is no information available about the structure underneath the hyaloclastitic body, we have not assigned a particular name to the deepest layer. Assuming a magnetization of 8 A m^{-1} for the outcropping tephrites and that hyaloclastites are not magnetized, we have deduced a magnetization value of 2 A m^{-1} for this body.

Conclusions

In this paper, we have presented a quantitative magnetic model of Vulcano based on high-resolution aeromagnetic data. The main purpose of this work was the modelling of the subsurface structure of the volcanic edifice beneath the two calderas. Appropriate selection of the profiles to be modelled, combined with previous geological and geophysical knowledge of this volcanic island, enabled a reliable magnetic interpretation to be made. In particular, rock magnetic properties based on paleomagnetic data and borehole stratigraphy obtained from two deep wells drilled inside the Fossa caldera constrained the modelling of the magnetic sources. Compared with previous geophysical works on the subsurface structure of Vulcano, our magnetic anomaly data set has allowed an optimum description of the anomalies linked to shallow buried structures beneath the whole of the volcanic edifice, including offshore areas. It is also worth noting the coherence between our models and the results obtained from other geophysical approaches. Nevertheless, it is important to be aware that, due to the intrinsic limitations of potential field interpretation, the actual structure beneath Vulcano might well differ to some extent from the models proposed here.

The interpretation of the modelled magnetic sources represents a significant contribution to the understanding of the structure beneath the two calderas of the Piano and the Fossa, providing us with evidence of the lateral discontinuity between them at depth. In particular, the magnetic pattern suggests the existence of an early volcanic phase solely beneath the Piano caldera, before the formation of the Primordial Vulcano. We suggest that the positive magnetic anomalies in the Piano caldera area have both a deep origin, related to the remnants of this early submarine volcano, and a shallow origin, linked to the feeding system of the Primordial Vulcano phase (beneath Mt. Saraceno) and to the presence of a non-outcropping dyke system intruded along an intra-caldera fault (beneath the eastern part of the Piano caldera). Offshore, to the west, the magnetic anomaly map revealed the presence of a submarine volcanic structure, which is not evident from bathymetric data. This volcanic body could represent the eruptive centre whose presence was deduced from the outcrop of eastern-dipping lavas in the western seashore. The modelling suggests that the eastern part of this body is covered by a large volume of almost non-magnetic material that could be interpreted as volcanoclastic sediments and also as pyroclastites pertaining to the subsequent phases of volcanic activity.

In the Fossa caldera, the magnetic modelling pointed to the presence of a highly magnetized cone-like body inside the Fossa cone, centred beneath the old crater. We interpret this body as a pile of mafic lavas emplaced in the early phase of activity of the Fossa cone, which would suggest that the volume of lavas erupted at the beginning of the construction of the Fossa was more important than has previously been deduced. In addition, the positive magnetic anomaly linked to this edifice implies that high temperatures in the cone must be limited to the fumarolic conduits and vents and cannot affect its bulk inner structure.

Structures beneath the western and northern part of the Fossa caldera are revealed to have null or low magnetization, which can be ascribed not only to the presence of pyroclasts and hyaloclastites in this area, but also to a large volume of hydrothermally altered materials. This result suggests that the hydrothermal system, with a very limited extension at present, affected a larger area in the past, especially beneath the western part of the caldera.

Acknowledgement We would like to thank Elena Zanella for providing us with unpublished paleomagnetic data and Guido Ventura, Claudia Romagnoli, and Franco Barberi for fruitful discussions on the volcanic history of Vulcano. We are also thankful to Jean-François Lénat for his careful review of the manuscript and to Maurizio Ripepe for editing it. Isabel Blanco-Montenegro was supported by the Spanish Ministry of Education and Science (Secretaría de Estado de Universidades e Investigación, Ayuda de Movilidad PR-2004-0201) and the Universidad de Burgos (Spain).

References

Ade-Hall JM, Palmer HC, Hubbard TP (1971) The magnetic and opaque petrological response of basalts to regional hydrothermal alteration. Geophys J R Astron Soc 24:137–174

Baranov V, Naudy H (1964) Numerical calculation of the formula of reduction to the magnetic pole. Geophysics 29:67–79

Barberi F, Innocenti F, Ferrara G, Keller J, Villari L (1974) Evolution of the Eolian arc volcanism (southern Tyrrhenian Sea). Earth Planet Sci Lett 21:269–276

Barberi F, Neri G, Valenza M, Villari L (1991) 1987–1990 unrest at Vulcano. Acta Vulcanol 1:95–106

Barberi F, Gandino A, Gioncada A, La Torre P, Sbrana A, Zenucchini C (1994) The deep structure of the Eolian arc (Filicudi–Panarea–Vulcano sector) in light of gravity, magnetic and volcanological data. J Volcanol Geotherm Res 61:189–206

Berrino G (2000) Combined gravimetry in the observation of volcanic processes in Italy. J Geodyn 30:371–388

Blanco-Montenegro I, Torta JM, Garcia A, Araña V (2003) Analysis and modelling of the aeromagnetic anomalies of Gran Canaria (Canary Islands). Earth Planet Sci Lett 206:601–616

Bonasia V, Luongo G, Montagna S (1973) A land gravity survey of the Aeolian Islands. Bull Volcanol 37:134–146

Budetta G, Nunziata C, Rapolla A (1983) A gravity study of the island of Vulcano, Tyrrhenian Sea, Italy. Bull Volcanol 46:183–192

Chiarabba C, Pino NA, Ventura G, Vilardo G (2004) Structural features of the shallow plumbing system of Vulcano Island Italy. Bull Volcanol 66:477–484

Chiodini G, Cioni R, Falsaperla S, Guidi M, Marini L, Montalto A (1992) Geochemical and seismological investigations at Vulcano (Aeolian Islands) during 1978–1989. J Geophys Res 97:11025–11032

De Astis G, Frazzetta G, La Volpe L (1989) I depositi di riempimento della Caldera del Piano e i depositi della Lentia. Boll GNV 2:763–778

De Astis G, La Volpe L, Peccerillo A, Civetta L (1997) Volcanological and petrological evolution of Vulcano island (Aeolian Arc, southern Tyrrhenian Sea). J Geophys Res 102(B4):8021–8050

De Astis G, Ventura G, Vilardo G (2003) Geodynamic significance of the Aeolian volcanism (southern Tyrrhenian Sea, Italy) in light of structural, seismological and geochemical data. Tectonics. DOI 10.1029/2003TC001506

De Ritis R, Blanco-Montenegro I, Ventura G, Chiappini M (2005) Aeromagnetic data provide new insights on the tectonics and volcanism of Vulcano island and offshore areas (southern Tyrrhenian Sea, Italy). Geophys Res Lett 32 (L15305). DOI 10.1029/2005GL023465

De Santis A, Gaya-Piqué L, Dominici G, Meloni A, Torta JM, Tozzi R (2003) Italian Geomagnetic Reference Field ITGRF: update for 2000 and secular variation model up to 2005 by autoregressive forecasting. Ann Geophys 46:491–500

Ellam RM, Hawkesworth CJ, Menzies MA, Rogers NW (1989) The volcanism of southern Italy: role of subduction and the relationship between potassic and sodic alkaline magmatism. J Geophys Res 94:4589–4601

Faraone D, Silvano A, Verdiani G (1986) The monzogabbroic intrusion in the island of Vulcano, Aeolian archipelago, Italy. Bull Volcanol 48:299–307

Favalli M, Karatson R, Mazzuoli R, Pareschi MT, Ventura G (2005) Volcanic geomorphology and tectonics of the Aeolian archipelago (southern Italy) based on integrated DEM data. Bull Volcanol 68:157–170

Finn CA, Morgan LA (2002) High-resolution aeromagnetic mapping of volcanic terrain, Yellowstone National Park. J Volcanol Geotherm Res 115:207–231

Frazzetta G, La Volpe L, Sheridan MF (1983) Evolution of the Fossa cone, Vulcano. J Volcanol Geotherm Res 17:329–360
Fulignati P, Gioncada A, Sbrana A (1999) Rare-earth element (REE) behaviour in the alteration facies of the active magmatic-hydrothermal system of Vulcano (Aeolian Islands, Italy). J Volcanol Geotherm Res 88:325–342
Gabbianelli G, Romagnoli C, Rossi PL, Calanchi N, Lucchini F (1991) Submarine morphology and tectonics of Vulcano (Aeolian Islands, southeastern Tyrrhenian Sea). Acta Vulcanol 1:131–141
Gillot PY, Frazzetta G, La Volpe L (1990) Volcanotectonic evolution of Vulcano (Aeolian Islands, southern Italy) from geochronological (K–Ar) study. Int Volcanol Congr (Mainz, September 3–8; abstract)
Gioncada A, Sbrana A (1991) “La Fossa caldera”, Vulcano: inferences from deep drillings. Acta Vulcanol 1:115–125
Gioncada A, Mazzuoli R, Bisson M, Pareschi MT (2003) Petrology of volcanic products younger than 42 ka on the Lipari–Vulcano complex (Aeolian Islands, Italy): an example of volcanism controlled by tectonics. J Volcanol Geotherm Res 122:191–220
Iacobucci F, Incoronato A, Rapolla A, Scarascia S (1977) Basement structural trends in the volcanic islands of Vulcano, Lipari, and Salina (Aeolian Islands, Southern Tyrrhenian Sea) computed by aeromagnetic and gravimetric data. Boll Geofis Teor Appl 20:73–74, 49–61
Italiano F, Nuccio PM, Valenza M (1984) Mass geothermal energy release at Vulcano, Aeolian Islands, Italy. Rend Soc Ital Mineral Petrol 39:379–386
Keller J (1974) Petrology of some volcanic rock series of the Aeolian Arc, southern Tyrrhenian Sea: calc-alkaline and shoshonitic associations. Contrib Mineral Petrol 45:29–47
Keller J (1980) The island of Vulcano. Rend Soc Ital Mineral Petrol 36:369–414
Keller J (1982) Mediterranean island arcs. In: Thorpe RS (ed) Andesites. Wiley, Chichester, pp 307–325
Lanza R, Zanella E (2003) Paleomagnetic secular variation at Vulcano (Aeolian Islands) during the last 135 kyr. Earth Planet Sci Lett 213:321–336
Lénat JF, Gibert-Malengreau B, Galdeano A (2001) A new structural model for the evolution of the volcanic island of Réunion (Indian Ocean). J Geophys Res 106(B5):8645–8663
Mazzuoli R, Tortorici L, Ventura G (1995) Oblique rifting in Salina, Lipari and Vulcano islands (Aeolian Islands, southern Italy). Terra Nova 7:444–452
Rasmussen R, Pedersen LB (1979) End corrections in potential field modelling. Geophys Prospect 27:749–760
Supper R, De Ritis R, Motschka K, Chiappini M (2004) Aeromagnetic anomaly images of Vulcano and southern Lipari Islands (Aeolian archipelago, Italy). Ann Geophys 47:1803–1810
Talwani M, Heirtzler JR (1964) Computation of magnetic anomalies caused by two-dimensional bodies of arbitrary shape. In: Parks GA (ed) Computers in the mineral industries, Part 1. Stanford Univ Publ Geological Sciences 9:464–480
Ventura G (1994) Tectonics, structural evolution and caldera formation in Vulcano island (Aeolian archipelago, southern Tyrrhenian Sea). J Volcanol Geotherm Res 60:207–224
Ventura G, Vilardo G, Milano G, Pino NA (1999) Relationships among crustal structure, volcanism and strike-slip tectonics in the Lipari–Vulcano volcanic complex (Aeolian Islands, southern Tyrrhenian Sea, Italy). Phys Earth Planet Int 116:31–52
Won IJ, Bevis M (1987) Computing the gravitational and magnetic anomalies due to a polygon: algorithms and Fortran subroutines. Geophysics 52:232–238
Zanella E, Lanza R (1994) Remanent and induced magnetization in the volcanites of Lipari and Vulcano (Aeolian Islands). Ann Geophys 37:1149–1156
Zanella E, De Astis G, Dellino P, Lanza R, La Volpe L (1999) Magnetic fabric and remanent magnetization of pyroclastic surge deposits from Vulcano (Aeolian Islands, Italy). J Volcanol Geotherm Res 93:217–236
Zanella E, De Astis G, Lanza R (2001) Palaeomagnetism of welded, pyroclastic-fall scoriae at Vulcano, Aeolian Archipelago. J Volcanol Geotherm Res 107:71–86